Distributed position sensing in bioinspired modular synchronous machines

Bryan Paul Ruddy
Auckland Bioengineering Institute
University of Auckland
Auckland, New Zealand
Email: b.ruddy@auckland.ac.nz

Matthew Nocete
Assurity Consulting
Wellington, New Zealand

Awhina Hona
Auckland Bioengineering Institute
University of Auckland
Auckland, New Zealand

***Abstract*—Modular and bioinspired architectures offer considerable promise for new motor designs. In some cases they may even offer unexpected benefits. Here, we first describe a bioinspired architecture for modular linear permanent magnet synchronous motors. We then focus on an additional use for the components of such a design, by constructing a distributed absolute position sensor within such a modular motor. By using a magnetic field sensor associated with each coil, and arranging the sensor outputs so that they are exponentially weighted or scaled from one end of the motor to the other, a unique absolute position signal can be obtained from a set of identical motor units.**

***Index Terms*—bioinspiration, motor cooling, sensing**

The quest for increasing force/torque density from electric motors often leads to consideration of unconventional designs and approaches. In general, there are two possible approaches on this quest: improving the motor constant, and thereby improving the efficiency of force/torque production; and improving heat transfer out of the motor, thereby increasing the amount of force/torque that can be produced. These two approaches can be at odds, however. Designs that increase heat transfer (e.g. [1]) often sacrifice efficiency by reducing fill factor or by weakening the magnetic field (e.g. [2]). It has been shown [3], [4] that the thermally-limited force/torque capability of a permanent magnet synchronous motor can be enhanced by reducing the characteristic dimension of the magnetic repeat unit, without altering the efficiency of force/torque production. However, if this scaling observation is exploited sufficiently to notably enhance motor performance, many challenges in fabrication and assembly of the resulting design arise.

We have been inspired to look to biology for approaches that might permit full exploitation of the scaling relationships governing synchronous motor performance. As shown in Fig. 1A, mammalian skeletal muscle is a multi-scale, modular structure, with nano-scale molecular motors (myosin traveling along actin) organised into microscale structures (sarcomeres) that are in turn combined in series to form milli-scale actuator units (muscle fibres) that are arranged in parallel to form fascicles and full-scale muscle-tendon units [5]. Muscle is densely populated with blood vessels that carry oxygen, heat, and metabolites [6] along with sub-cellular mitochondrial networks for energy [7]. Nerves and T-tubules [8] accomplish a similar function with a similar architecture for control signals.

The architecture of muscle has inspired us to consider a modular approach to motor design, with small, identical repeat units comprising magnets, coils, power electronics, and cooling systems assembled in series and parallel to build up a linear synchronous motor of the desired stroke length and force capability as shown in Fig. 1B. While there has been some previous exploration of modular motors designed according to these principles [10], it has not been explored with efficiency as a key outcome. A modular muscle-inspired motor design approach has the potential to both balance thermal and electromagnetic performance constraints and to allow exploration of novel control strategies, such as independent control of all coils and/or recruitment-based control approaches. It also can manage fabrication challenges by utilizing mass-produced identical modules.

In this paper, we will investigate one facet of our proposed bioinspired modular design approach: can an architecture of repeated identical segments offer the ability to determine the absolute motor position, without adding an external position sensor? We will describe the basis of such a position sensing scheme, including simulation results verifying the potential for an appropriate design to yield a robust position estimate, as well as verification using experimental data.

I. Sensor design approach

In order to design a position sensor, we must first digress slightly and discuss how such a modular synchronous motor would be controlled. Fig. 2 provides a conceptual view of the different components needed as part of a motor module, including a movable magnet, a fixed stator coil, and an electrical circuit to control the coil. The magnet and stator components need not have the same repeat length in this architecture. This module can function autonomously if it is equipped with a magnetic field sensor, logic circuits, and appropriate power switches, so that the coil current can be set appropriately to generate force based on the measured magnetic field being experienced by the coil. A motor made of such modules would function as though it had a very high phase count, with the

This work has been supported by the Marsden Fund Council from New Zealand Government funding, managed by Royal Society Te Apārangi.

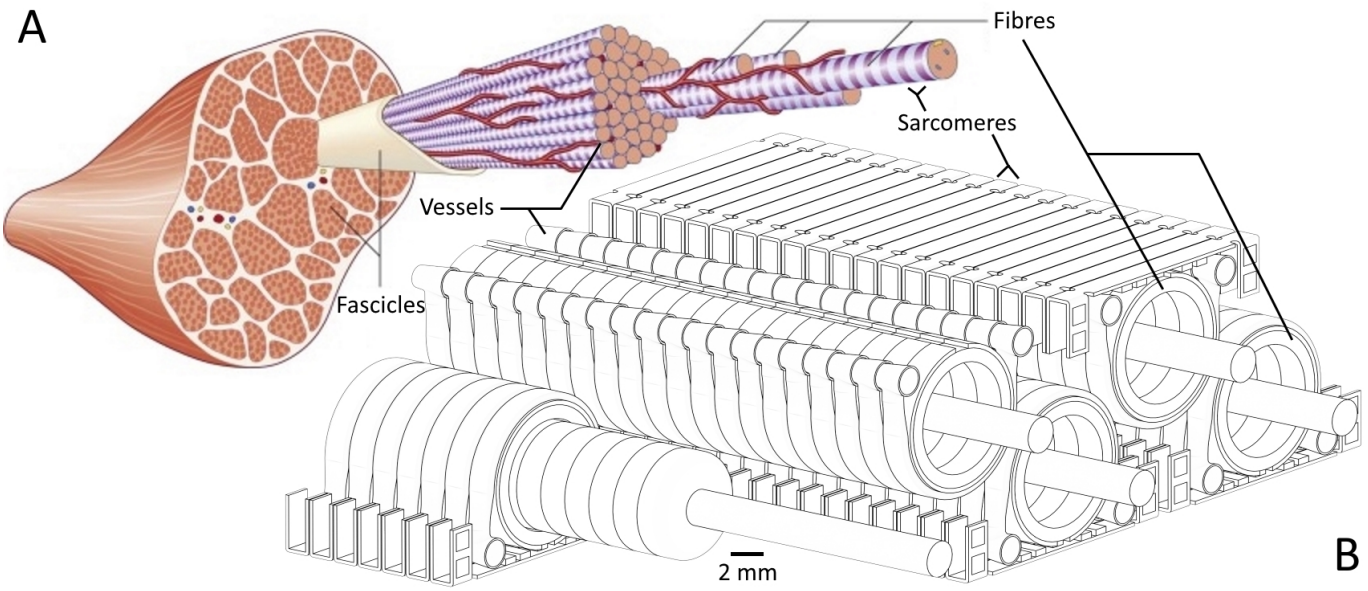

Fig. 1. A: The hierarchical structure of skeletal muscle. (Figure adapted from [9].) B: Our proposed hierarchical electric motor structure, with scale bar below.

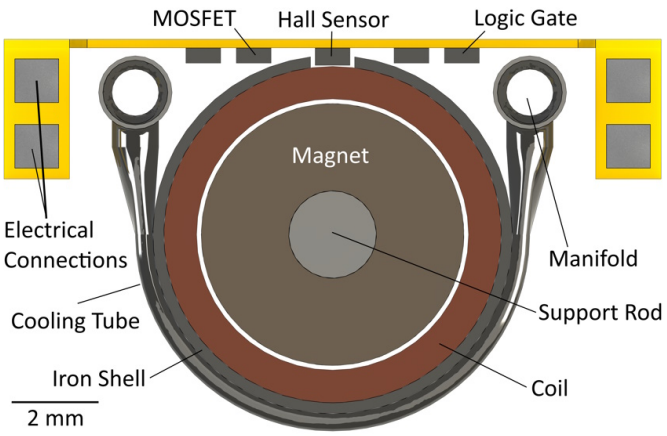

Fig. 2. The proposed modular tubular motor unit.

coil current waveform very closely aligned to the magnetic field.

This basic architecture offers two major design choices: digital or analog field sensing? Trapezoidal or sinusoidal commutation?

The presence of a magnetic field sensor also invites the design of a position sensor. In typical three-phase synchronous motors, a set of three magnetic field sensors is commonly used as an incremental position sensor and commutation controller. However, in this modular architecture, we already have a very large number of sensors available from the distributed commutation. In particular, this motor architecture invites the use of a short-magnet (overhung) design, where the coils not exposed to the field from the moving magnet are automatically quiescent and not driven by their local power electronics; in an overhung design, the total set of coils is provided with enough information to determine the absolute mover position, not just an incremental position.

What remains is the problem of breaking the periodicity of the motor to give it a "front" and a "back," for determining absolute position. Conceptually, this can be done by including a transmission line, delay line, or even just impedance through the repeat units, such that a signal introduced at one end of a motor assembly is delayed and/or attenuated by the time it reaches the opposite end.

Based on these factors, we considered three sensor architectures, shown in Fig. 3. In all of these architectures, an analog magnetic field sensor is used, such as an amplified Hall element. In the first one, the sensor voltages are scaled by a linearly-varying factor, and all scaled sensor voltages are summed. In the second, the sensor voltages are scaled by an geometrically-scaled factor, produced by a resistor ladder, before summing. In the third, and much simpler, architecture, the sensor output voltages directly feed into a resistor ladder. While we have shown these designs implemented as analog circuits, the same effect can be achieved digitally within each module. In all architectures, we further require that there are two outputs, and that rather than all sensors being connected the modules are wired so that even modules contribute to channel "A" and the odd modules contribute to channel "B."

II. Theory and Simulation

Each channel in each of the three sensor architectures in Fig. 3 can be mathematically described as the summation of a series of position measurements V_i to find an output value V_{out}:

$$V_{\text{out}} = C \sum_{i=1}^{n} \alpha_i V_i, \tag{1}$$

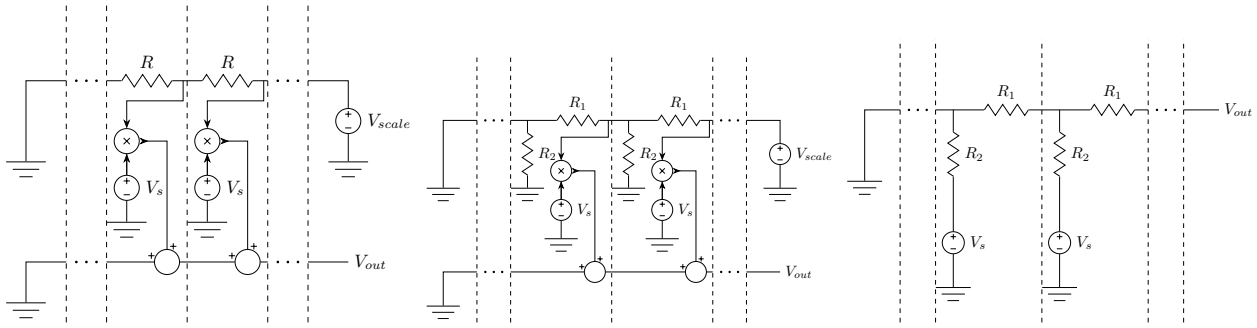

Fig. 3. Sensor architectures: Left – Linear scaling. Centre – Geometric scaling. Right – Resistive adding. In all three figures, V_{s} is the individual sensor voltage, V_{out} is the output voltage, and V_{scale} is an arbitrary scaling voltage.

where the architectures differ in the coefficients α_i and in the overall scale C. Here, n is the number of modular units in the system, and relative to the depictions in Fig. 3 the module for which $i = 1$ is on the left. In the linear scaling approach and the geometric scaling approach, the overall scale parameter $C = 1$, and the coefficients are given by $\alpha_i = iV_{\mathrm{scale}}/n$ and by $\alpha_i = V_{\mathrm{scale}}/r^{n-i-1}$, respectively, where $r \equiv R_1/R_2$.

The derivation of the coefficients for the passive resistive adding network is more complex. The scale parameter is given by $C = 1 + \sum_{i=1}^{n} \alpha_i$, and the coefficient is given recursively by

$$\alpha_i = \alpha_{i-1} + r\left(1 + \sum_{j=1}^{i-1} \alpha_j\right), \tag{2}$$

where $\alpha_1 = r$. This relationship can be closely approximated by an exponential function, $\alpha_i = \mathrm{e}^{\gamma i}$, where γ is given by a curve fitting process as

$$\gamma \approx 0.9788 r^{0.4746} - 0.0123 \tag{3}$$

with an RMS error of less than 0.02.

Initial MATLAB simulation of the behaviour of the linear and geometric scaling functions is shown in Figs. 4 and 5. The linear scaling (Fig. 4) is insufficient to break the symmetry of the motor, and no discernible relationship between the two channels and the position of the magnet in the motor can be found. However, the geometric scaling (Fig. 5) does provide a unique relationship between the two channel voltages and the position, as shown by the failure of the line to cross itself. The shape of this curve nonetheless suggests a strong sensitivity to noise, as relatively little noise would be required to drive the curve to self-cross.

Encouraged by the initial geometric scaling results, we then conducted a simulation campaign in Python to determine the influence of the sensor spacing and resistor ratio upon the sensor output characteristics, and to investigate methods for finding the position from the two signals. For example, Fig. 7 shows the sensor outputs for $r = 0.01$ and $r = 0.1$, for a magnet 5 repeat units long, a coil structure double that length, and sensors spaced 60 mechanical degrees apart.

We then converted the A and B channel data to polar coordinates, centred on the top right corner of the signals, and performed a linear fit between the logarithm of the radius and the displacement. This simple approach still leaves significant residual error, but illustrates that the absolute position can be calculated via this technique.

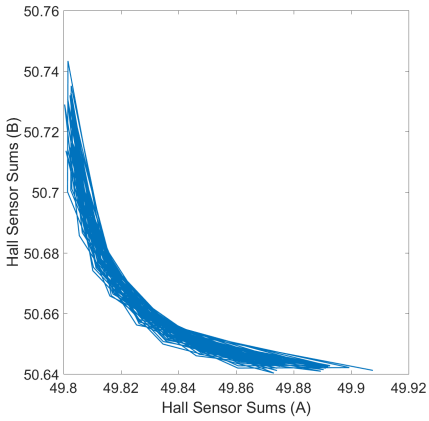

Fig. 4. Sensor outputs when used with linear scaling.

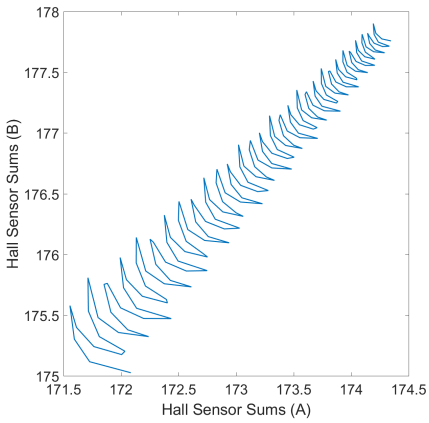

Fig. 5. Sensor outputs when used with geometric scaling.

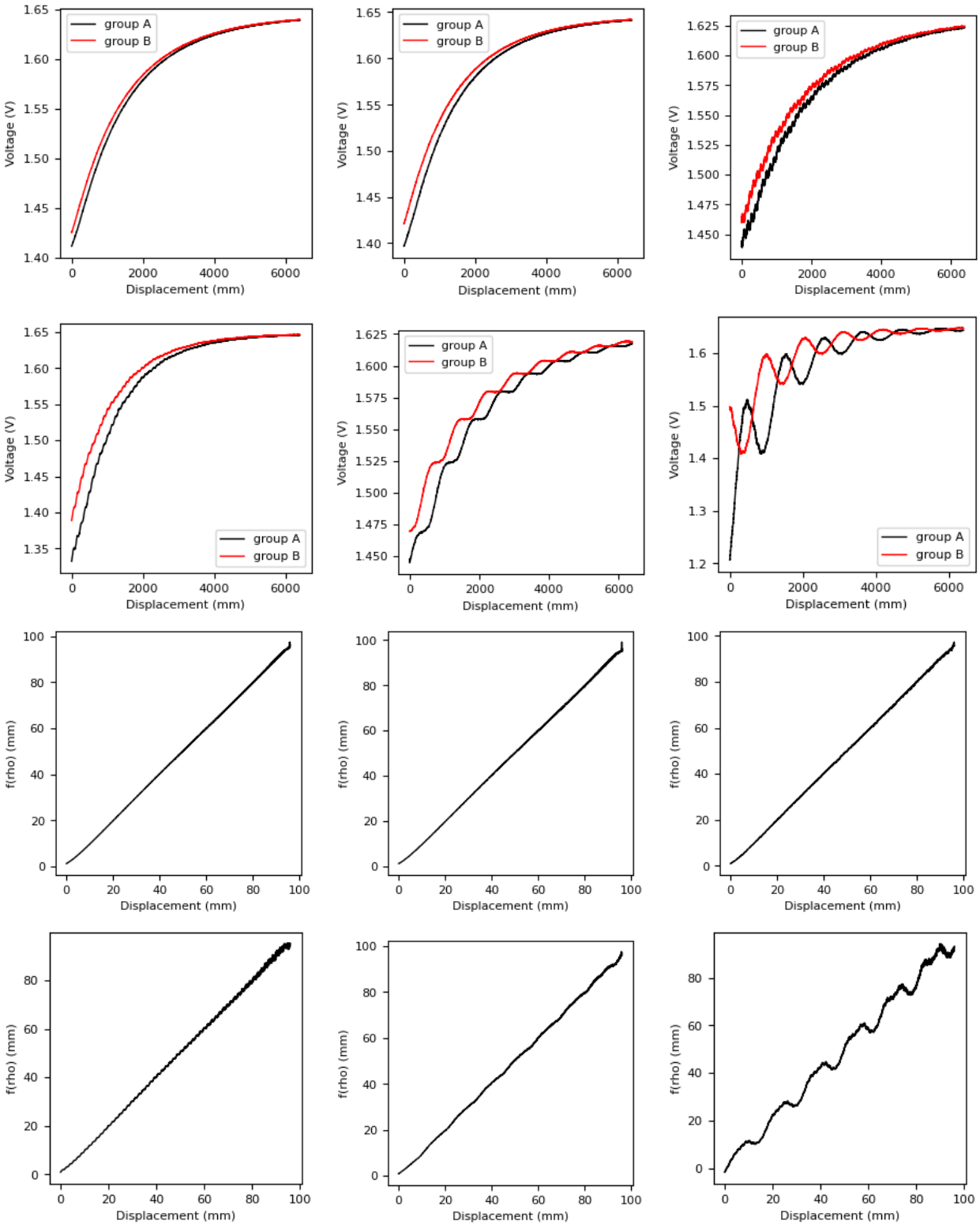

Fig. 6. Emulated output voltages and fit results at six sensor spacings. Top row: 30°, 45°, 60°. Second row: 72°, 90°, 120°. Third row: 30°, 45°, 60°. Bottom row: 72°, 90°, 120°.

III. Experimental results

We constructed a test circuit and magnet array to verify the method with experimental data. As shown in Fig. 8, we constructed a magnet array from 25 mm by 9 mm by 3 mm, N45 grade magnets (Magnets NZ Ltd), spaced to form an array

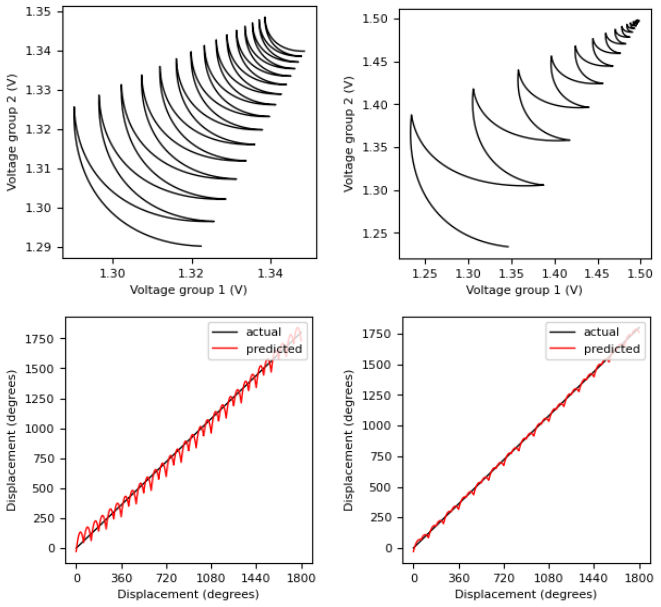

Fig. 7. Top: Sensor outputs for the passive adding network, with $r = 0.01$ on the left and $r = 0.1$ on the right. Bottom: The predicted position for each sensor configuration, determined by converting the two sensor values to a radius and taking its logarithm.

with a 24 mm repeat length and four repeats (96 mm total length) on a steel backing plate. The array was mounted to a motorised linear stage. Above the stage, we placed an array of four analogue Hall effect sensors (Allegro Microsystems A1391) spaced 6 mm apart. (Only one sensor was used to obtain the subsequent results.) The magnetic field was scanned over a total length of 288 mm, centred on the magnet array, with 1000 samples (National Instruments USB-6361, 10 kHz sample rate) taken at each point and measurement points spaced 0.015 mm apart. All 1000 samples were averaged to a single value per measurement point to reduce noise.

Data from one sensor were processed to emulate the output of a sensor array 192 mm long, at various sensor spacings. The emulated channel voltages were then processed by fitting a fourth-order polynomial model to the logarithm of the radius, as described above, and compared to the actual position.

The results of this experiment are summarised in Fig. 6. At each sensor spacing except for 120°, we were able to find a value of r that led to a high-quality position fit, with the RMS error under 1 mm. The role of r is shown in Fig. 9 - at each position, there is a wide range of r values that can lead to good estimates.

IV. Conclusion and Future Works

We have described a new architecture for distributed motor position sensing, and presented preliminary simulation and experimental results to demonstrate the feasibility of this approach. In the future, we will construct a full-scale sensor array to fully validate the approach, and investigate additional noise sources that can arise during motor operation.

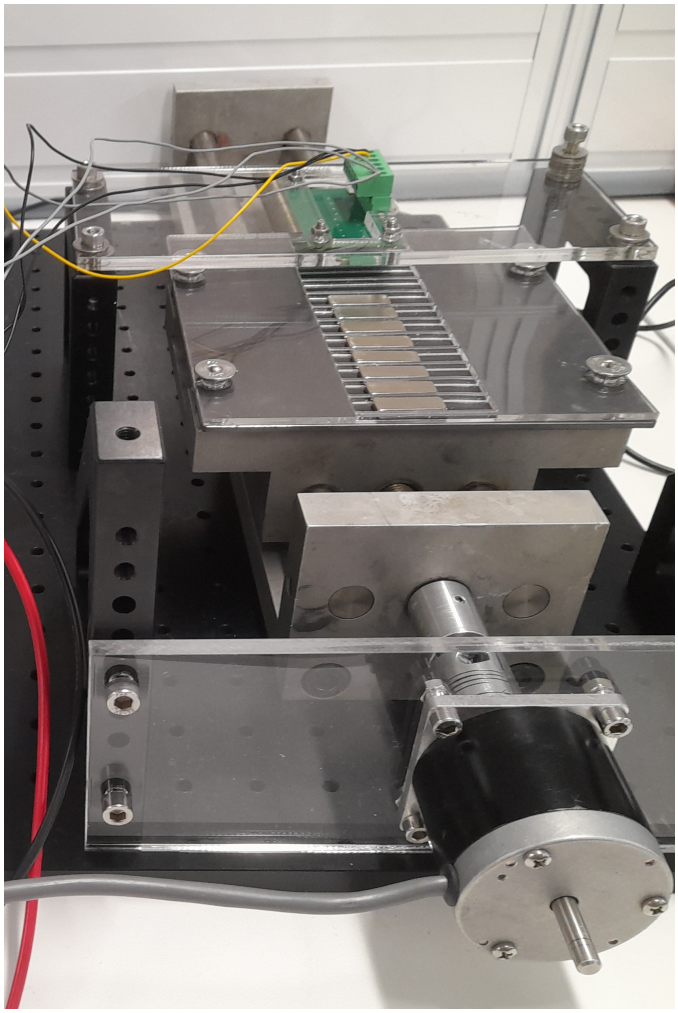

Fig. 8. Experimental apparatus: a pcb-mounted sensor array above a magnet array, mounted on a motorised linear stage.

References

[1] M. K. Liebman, "Thermally efficient linear motor analysis & design," Master's thesis, Massachusetts Institute of Technology, Feb. 1998.

[2] B. P. Ruddy, *High force density linear permanent magnet motors: "Electromagnetic muscle actuators"*. PhD thesis, Massachusetts Institute of Technology, 2012.

[3] B. P. Ruddy and I. W. Hunter, "Design and optimization strategies for muscle-like direct-drive linear permanent-magnet motors.," *The International Journal of Robotics Research*, vol. 30, no. 7, pp. 834–845, 2011.

[4] B. Hannaford, P.-H. Marbot, P. Buttolo, M. Moreyra, and S. Venema, "Scaling of direct drive robot arms," *The International Journal of Robotics Research*, vol. 15, no. 5, pp. 459–472, 1996.

[5] F. E. Zajac, "Muscle and tendon: Properties, models, scaling, and application to biomechanics and motor control," *Critical Reviews in Biomedical Engineering*, vol. 17, no. 4, pp. 359–411, 1989.

[6] O. Mathieu-Costello, "Comparative aspects of muscle capillary supply," *Annual review of physiology*, vol. 55, no. 1, pp. 503–525, 1993.

[7] B. Glancy, L. M. Hartnell, D. Malide, Z.-X. Yu, C. A. Combs, P. S. Connelly, S. Subramaniam, and R. S. Balaban, "Mitochondrial reticulum for cellular energy distribution in muscle," *Nature*, vol. 523, no. 7562, p. 617, 2015.

[8] T. Hong and R. M. Shaw, "Cardiac T-tubule microanatomy and function," *Physiological reviews*, vol. 97, no. 1, pp. 227–252, 2017.

[9] S. Standring, ed., *Gray's anatomy: the anatomical basis of clinical practice*. New York: Elsevier, 41 ed., 2016.

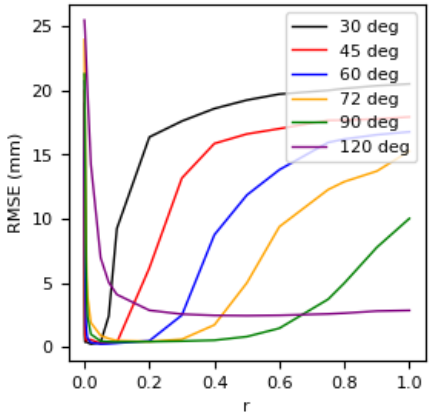

Fig. 9. The relationship between the resistor ratio and the quality of position estimate.

[10] G. Mathijssen, J. Schultz, B. Vanderborght, and A. Bicchi, "A muscle-like recruitment actuator with modular redundant actuation units for soft robotics," *Robotics and Autonomous Systems*, vol. 74, pp. 40–50, 2015.